

INFLUENCE OF TARGET SPAN AND CONFIGURATION ON BALLISTIC RESISTANCE OF DUCTILE MATERIAL

G.Tiwari, M.A. Iqbal, P.K.Gupta

Department of civil engineering, Indian Institute of Technology Roorkee, Roorkee 247667, India

Abstract

The three dimensional numerical simulations had been carried out to investigate the influence of target span and configuration on ballistic resistance of thin aluminum target plate. 1mm thick 1100-H12 aluminum target plate was hit by 19 mm diameter ogive nosed projectile. The span was varied as 50, 76, 100, 255 and 760 mm whereas the configuration of 255 mm span diameter target was varied as 1 mm thick monolithic, double layered in-contact (2 x 0.5 mm) and double layered spaced. The spacing between the layers was also varied as 2, 5 and 10mm. The target was impacted normally by ogive nosed projectile to obtain the ballistic limit, failure mode and deformation. Johnson–Cook elasto-viscoplastic constitutive model was considered to simulate the material behavior of 1100-H12 aluminum. The ballistic limit was found to increase with an increase in span diameter. The monolithic target offered highest ballistic limit followed by layered in-contact and spaced targets respectively. The variation of spacing between the layers did not have significant influence on the ballistic limit.

Keywords: Span Diameter, Layered Target; Spaced Target; Ogive Nosed projectile

Introduction

Design of metal shields for protection against projectiles impact has long been of interest in military and civilian applications. Penetration and perforation related problems have been studied for a long time, and substantial efforts have been made by experimental, numerical and theoretical investigations in order to understand the phenomena occurring in the target impacted by projectile. When a single plate is replaced by several layered thin plates, the order, thickness, number of layers and the air gap between layers affect the failure models, which lead to the difference of the ballistic resistance between various configuration targets. Although there were a number of studies dealing with the ballistic behavior of multi-layered plates, but their scope was limited when compared to studies of monolithic plates.

Gupta et al [1] studied the perforation behavior of thin aluminum plate experimentally as well as numerically by hitting the blunt and hemispherical nose projectile on 1mm thick aluminum plate. Blunt projectile was found to be better penetrator as compare to spherical nosed projectile. With the help of smooth and notched tensile test specimens the tests were performed to carry out the material property. Iqbal et al [2] carried out the numerical study to know the impact behavior of ductile targets subjected to normal and oblique impact by sharp nosed cylindrical projectiles. Weldox 460 E steel plate of 12 mm thickness and 1mm thick 1100-H12 aluminum plate was hit normally and at some oblique angle by conical nosed projectile and ogive nosed projectile respectively. There is sharp change in ballistic resistance of steel target after 30° obliquity, whereas for aluminum the ballistic limit continuously increased with obliquity. Arias el al. [3] also investigated the perforation behavior of thin steel plates impacted by blunt, conical and hemispherical nosed projectile with a large range of impact velocities from 190 to 600 m/s. It has been found that for blunt projectile impact target fails mainly due to adiabatic shear band propagation which results ejection of plug, for conical projectiles impact target fails due to hole enlargement whereas in case of hemispherical impact material becomes thin due to compressive stress and a small thin plug separates from target material.

Gupta et al. [4, 5] carried out experimental and numerical investigations of thin single and layered aluminum targets impacted normally by blunt, ogive and hemispherical nosed projectiles. Effect of projectile nose shape, impact velocity and target thickness on the ballistic resistance was studied. For thin plates (0.5, 0.71, 1.0 and 1.5 mm) ogive nosed projectile was

found to be the more efficient penetrator. For thicker plates (2.0, 2.5 and 3.0 mm) however, blunt nosed projectiles required lesser resistance against perforation. In the case of layered in contact targets ogive nosed projectile was found to be the most efficient penetrator. Hemispherical nosed projectile remained least efficient to perforate both single as well as layered targets.

Corran et al. [6] studied the effect of projectile mass, nose shape, and hardness on the penetration resistance of steel and aluminum targets. Experiments carried out in the sub-ordinance velocity range showed that an increase in the projectile nose radius changes the failure mode from ductile hole enlargement (by wedge nosed projectile) to thinning due to tensile stretching (by hemispherical nosed projectile) and shearing of target (by blunt nosed projectile). The failure of target for nose radii of 6.25 mm (hemispherical) and 9.5 mm occurred by tensile stretching and considerable out of plane deflection (up to 13 mm). For nose radii in excess of 12 mm the plate failure occurred through plugging. Plate deformation decreased with increasing nose radius. The peak perforation energy occurred for a nose radius of 11 mm that was about four times higher than that observed for blunt nosed projectile. Dean et al. [7] concerned with energy absorption in thin (0.4 mm) steel plates during perforation by spherical projectiles of hardened steel; at impact velocities between 200 and 600 m/sec. Absorbed energies have been obtained from measured incident and emergent projectile velocities. These tests were simulated using ABAQUS/Explicit, using the Johnson and Cook plasticity model. A strain rate-dependent, critical plastic strain fracture criterion was employed to model fracture. Good agreement is obtained between simulations and experiment and the model successfully captures the transitions in failure mode as projectile velocity increases. At velocities close to the ballistic limit, the plates fail by dishing and discing. As the incident velocity is increased, there are two transitions in failure mode, firstly to shear plugging and secondly to fragmentation and petalling. The simulations also show that, during the latter mode of failure, the kinetic energy of ejected debris is significant, and failure to include this contribution in the energy balance leads to a substantial over-estimate of the energy absorbed within the sheet.

The subject of target configuration has been studied in literature by varying the number of in-contact as well as spaced layers. The order of layering of the plates with different thicknesses and material has also been studied. However, available studies have disagreement regarding the efficiency of monolithic, layered and spaced targets. The influence of projectile nose shape on

target configuration is also not clear and requires more investigation. On the other hand there is hardly any study wherein the span of the target has been varied to understand its effect on the ballistic limit.

The present numerical study describes the effect of target span diameter and configuration on the ballistic limit. 1 mm thick monolithic 1100-H12 aluminum targets of span diameters 50 mm, 76 mm, 100 mm, 255 mm and 760 mm were impacted by ogive nosed projectiles to obtain ballistic limit. The configuration of 255 mm span diameter target was also varied as monolithic, double layered in-contact and double layered spaced of equivalent thickness 1 mm. Spacing between the layers was varied as 2 mm, 5 mm and 10 mm. The target with varying configuration was also impacted by ogive nosed projectile in order to obtain ballistic limit. To study the influence of target span, impact velocities of projectiles were kept identical to those obtained during experiments carried out by Gupta et al. [5] on 1 mm thick monolithic target. To study the influence of target configuration, impact velocities of projectiles were kept identical to those obtained during experiments carried out by Gupta et al. [5] on 0.5 mm thick double layered in-contact target. In general the ballistic limit was found to increase with an increase in target span diameter. Monolithic targets were found to offer highest ballistic limit followed by layered in-contact and layered spaced targets of equivalent thickness.

Constitutive Modeling

A metal plate subjected to projectile impact is a very complex phenomenon due to yielding, plastic flow, isotropic strain hardening, strain rate hardening, softening due to adiabatic heating and damage. Johnson–Cook elasto-viscoplastic constitutive model [9, 10] that considers the all above effect of linear thermo-elasticity, is used to simulate the material behavior of 1100-H12 aluminum. Table 1 shows the material parameter for 1100-H12 aluminum.

The equivalent von-Mises stress for the Johnson–Cook model is expressed in the following form;

$$\bar{\sigma} = [A + B(\bar{\epsilon}^{pl})^n][1 + C \ln\{\frac{\dot{\bar{\epsilon}}^{pl}}{\dot{\bar{\epsilon}}_0}\}][1 - \hat{T}^m] \quad (1)$$

while the failure strain is expressed by

$$\bar{\epsilon}^{pl}(\frac{\sigma_m}{\bar{\sigma}}, \dot{\bar{\epsilon}}^{pl}, \hat{T}) = [D_1 + D_2 \exp(D_3 \frac{\sigma_m}{\bar{\sigma}})][1 + D_4 \ln(\frac{\dot{\bar{\epsilon}}^{pl}}{\dot{\bar{\epsilon}}_0})][1 + D_5 \hat{T}] \quad (2)$$

$$\hat{T} = (T - T_0)/(T_M - T_0) \quad (3)$$

where T is the current temperature, T_M is the melting temperature, T_0 is the room temperature, A is quasi-static yield stress, B is a hardening constant, n is the hardening exponent, C is the strain rate sensitivity parameter and m is the temperature sensitivity parameter. $\bar{\epsilon}^{pl}$ is the equivalent plastic strain, $\dot{\bar{\epsilon}}^{pl}$ is equivalent plastic strain rate, $\dot{\bar{\epsilon}}_0$ is a reference strain rate, D_1 – D_5 are material parameters, $\frac{\sigma_m}{\sigma}$ is the stress tri-axiality ratio and σ_m is the mean stress.

Modeling details

The three dimensional finite element model of the projectile and target was made using ABAQUS/CAE as shown in Fig. 1. The projectile was modeled as rigid and the target as deformable body. The Johnson-Cook constitutive model which is inbuilt in ABAQUS finite element code was used to model the material behavior of 1100-H12 aluminum. The kinematic contact algorithm was considered to define the contact between the projectiles and target whereas general contact algorithm was used to define the contact between the contacting surfaces of layered in-contact target. The outer surface of the projectile was modeled as the master surface and the contact region of the target as node based slave surface. The rear surface of front layer was considered as master surface and front surface of rear layer was considered as the slave surface. The targets were restrained at its periphery with respect to all degrees of freedom to model its periphery fixed. 8-node brick elements were considered for meshing the target plate. FE results influence by mesh density in impact zone. Mesh convergence study already completed [2] according to which for 1mm thickness plate there should be six elements across the thickness. In 1mm thickness plate the element size will be $0.16 \times 0.16 \times 0.16$ mm mesh size in impact zone. Dynamic explicit method was used to solve the impact phenomenon.

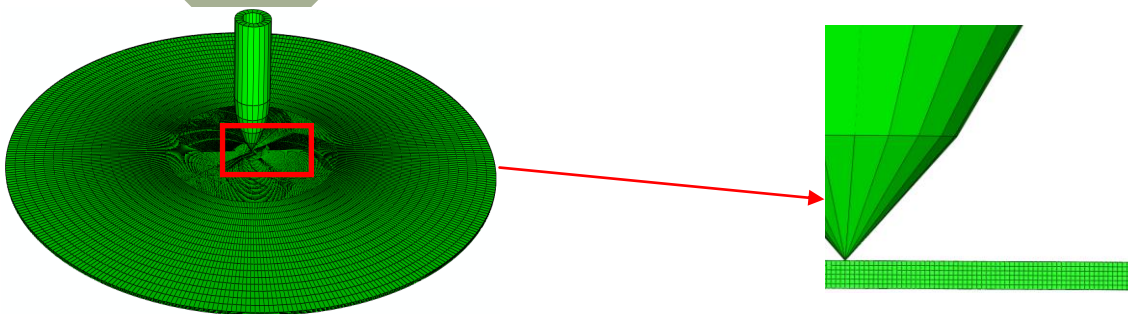


Figure 1: Finite element model for normal impact of ogive nosed projectile

Results and Discussion

The results of the present numerical study for varying target configuration are shown in Table 2 in the form of impact and residual velocities of ogive nosed projectiles. The projectile was impacted normally on 1 mm thick targets which were monolithic, double layered in contact and double layered with different spacings.

Monolithic target offered highest ballistic limit followed by layered in-contact and layered spaced targets respectively for both the projectiles. The results for varying span diameter are presented in Table 3 in the form of impact and residual velocities of ogive projectiles. It was observed that the ballistic limit of target increases with an increase in span diameter. compares the results of present three-dimensional numerical study with the experimental and axi-symmetric numerical studies carried out by Gupta et al. [5] on double layered 0.5 mm thick plates in-contact. The ballistic limit of this target was found to be 48.0 m/s from the present numerical simulation and 46.9 m/s from the experiments. Fig. 3 compares the results of present numerical study with experiments and axi-symmetric numerical simulations carried out by Gupta et al. [5] for 1 mm thick monolithic target of 255 mm span diameter. For ogive nosed projectile the ballistic limit of target was found to be 54 m/s from the present numerical study and 48.2 m/s from the experiments.

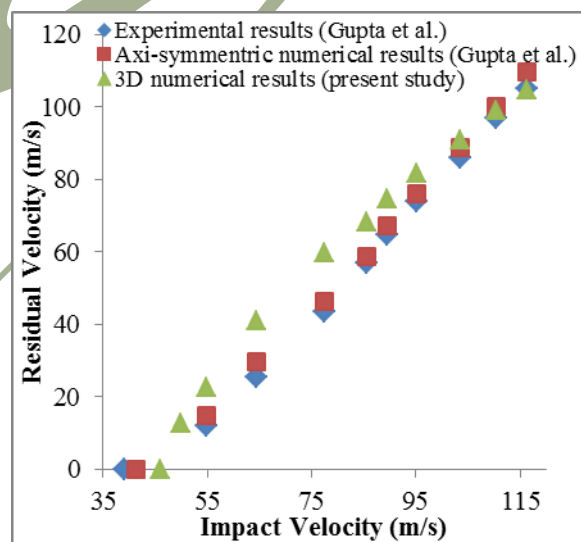


Figure 2: Comparison of present three-dimensional numerical results with the previous experimental and axi-symmetric numerical studies for 0.5 mm thick double layered 1100-H12 aluminum target impacted by ogive nosed projectile

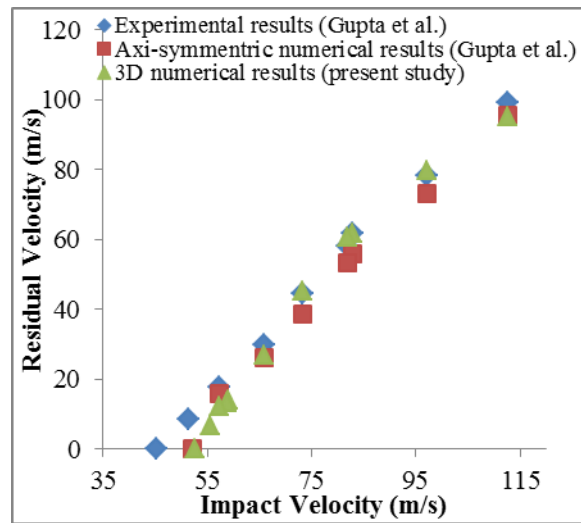


Figure 3: Comparison of present three-dimensional numerical results with the previous experimental and axi-symmetric numerical studies for 1 mm thick monolithic 1100-H12 aluminum target impacted by ogive nosed projectile

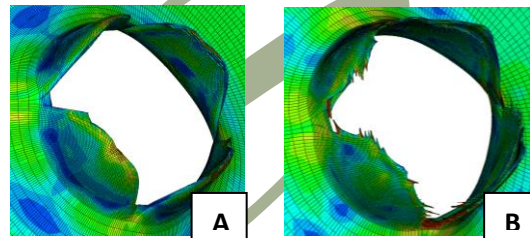


Figure 4: Fracture modes of (A) 1 mm thick monolithic and (B) 0.5 mm thick double layered target impacted by ogive nosed projectile.

Fig. 4 shows the failure mode of 1 mm thick monolithic and 0.5 mm thick double layered in-contact targets impacted by ogive nosed projectile. The projectile caused failure through ductile hole enlargement and petal formation. This is a typical failure mode of thin ductile targets impacted by sharp nosed projectiles. Four equal petals were formed in single, layered as well as spaced targets of equivalent thickness. Petals were bent at 90° from the surface of target for each configuration. Petals were found to be highly sharp and thin at their tip, thickness increased from the tip to the root of petals. Experiments [4,5] also revealed that four equal petals were formed in 1 mm thick monolithic and 0.5 mm thick double layered in-contact targets when impacted by ogive nosed projectiles.

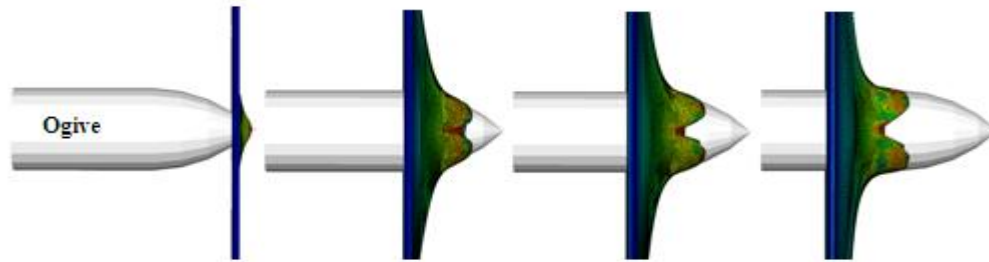


Figure 5: Perforation of 1 mm thick monolithic target by ogive nosed projectiles

Fig. 5 shows the perforation phenomenon of 1 mm thick monolithic targets impacted by ogive nosed projectiles. The phenomena of ductile hole enlargement and petal formation by ogive nosed projectile can be seen.

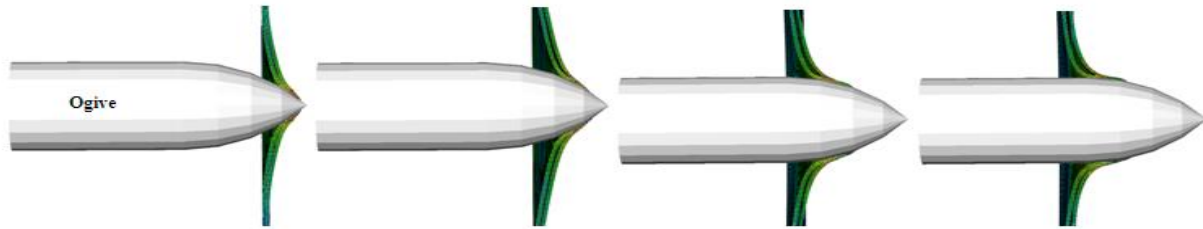


Figure 6: Perforation of 0.5 mm thick double layered in-contact targets by ogive nosed projectiles

Fig. 6 shows the perforation behavior of layered in-contact targets impacted by ogive nosed projectiles. The deformation as well as fracture mode of layered targets was identical to those of the monolithic targets impacted by respective projectiles. The layers were in contact before the commencement of fracture, however, as the fracture started both the layers separated with each other.

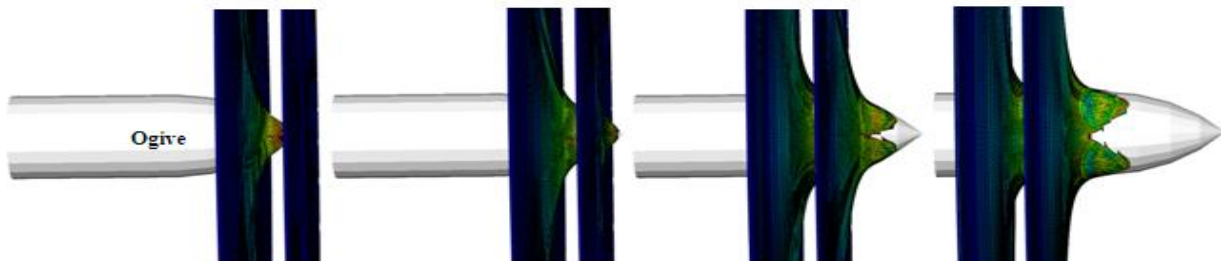


Figure 7: Perforation of 0.5 mm thick double layered target with 10 mm spacing by ogive nosed projectiles

Fig. 7 shows the perforation of double layered target with 10 mm spacing between the layers. In this case also the failure mode of target remained identical to that of the monolithic and layered in-contact target for respective projectiles. It can be seen that there is a contact established between the front and rear layer as the projectile deforms the front layer. This phenomenon occurred for 2 mm, 5 mm and 10 mm spaced target. However, the contact between layers was defined for all the cases of spaced targets.

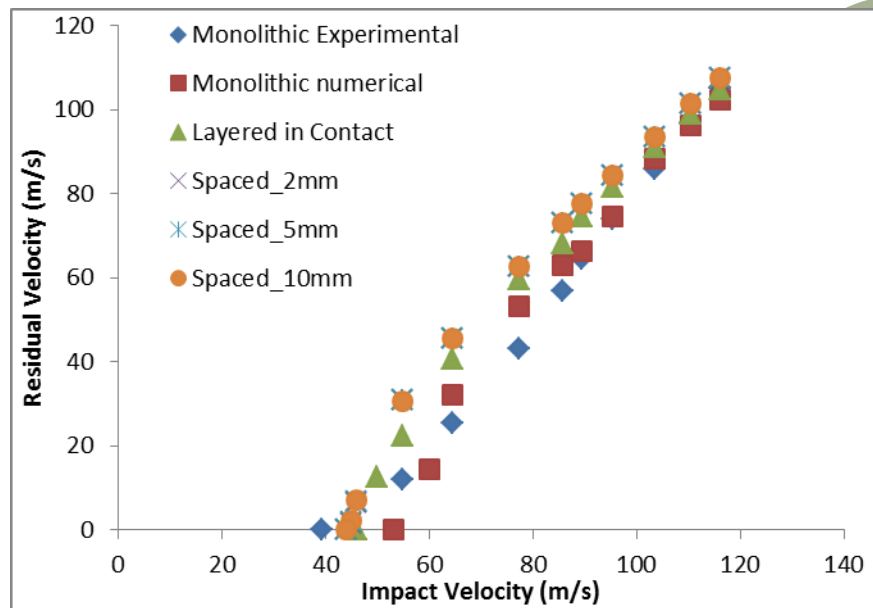


Figure 8: Impact and residual velocity curves for 1 mm thick monolithic, 0.5 mm thick double layered in-contact and 0.5 mm thick double layered spaced targets impacted by ogive nosed projectile

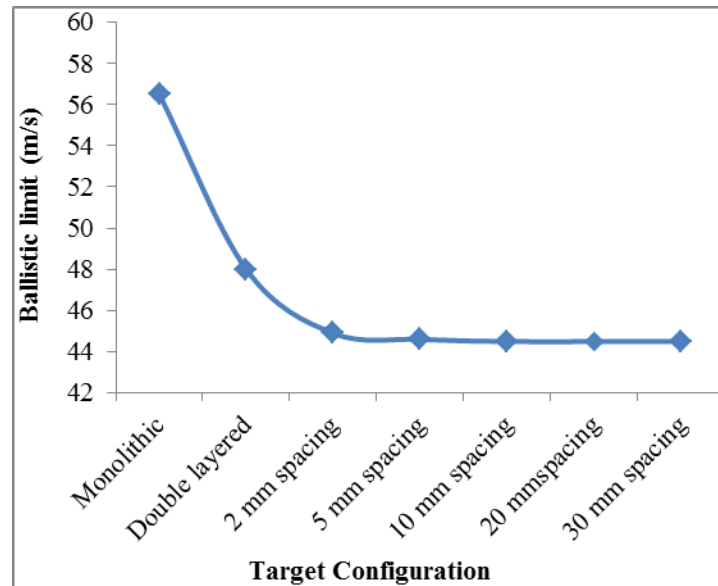


Figure 9: Variation of ballistic limit with target configuration of 1 mm equivalent thickness ogive nosed projectile

Fig. 8 shows the residual velocity corresponding to different impact velocity for different configurations. The variation of ballistic limit with target configuration is plotted in Fig. 9. It was found that the ballistic limit of monolithic target was found to be highest followed by layered in-contact and layered spaced target respectively. The spaced targets were found to be least effective. For ogive nosed projectile the ballistic limit of monolithic target was found to be 17.7% and 25.8% higher than that of the double layered in-contact and 2 mm spaced target respectively. The ballistic limit of layered in-contact target was found to be 7% higher than that of the 2 mm spaced target. While the ballistic limit of spaced target remained almost identical at varying spacing.

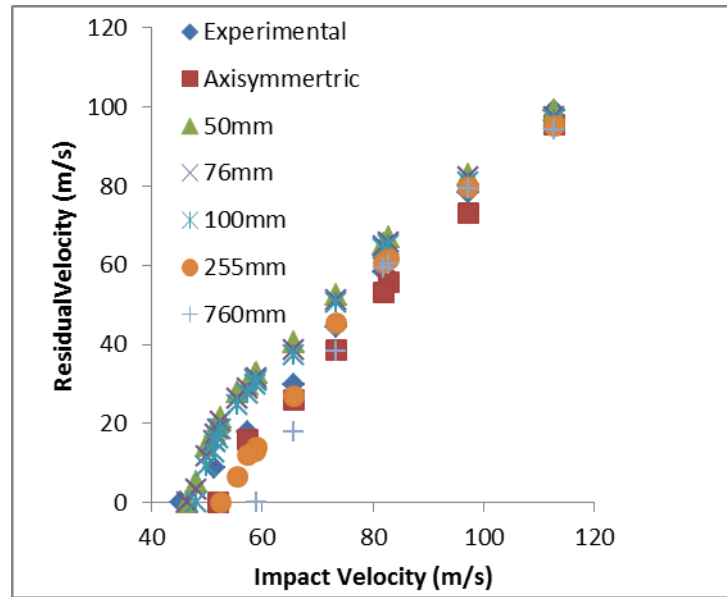


Figure 10: Comparison of impact and residual velocities for varying span diameter of 1 mm thick monolithic target impacted by ogive nosed projectile

Figs. 10 shows impact and residual velocity curves of ogive nosed projectiles respectively for 50 mm, 76mm, 100 mm, 255 mm and 760 mm span diameters. Results reveal that at higher impact velocities the increase in the resistance offered by target of larger span is not significant. However, with decrease in the impact velocity, targets with larger span diameter were found to offer significant increase in resistance. This behavior was seen to be more prominent at the ballistic limit, Table 5. Increase in ballistic limit for ogive nosed projectiles may be seen in Fig. 11.

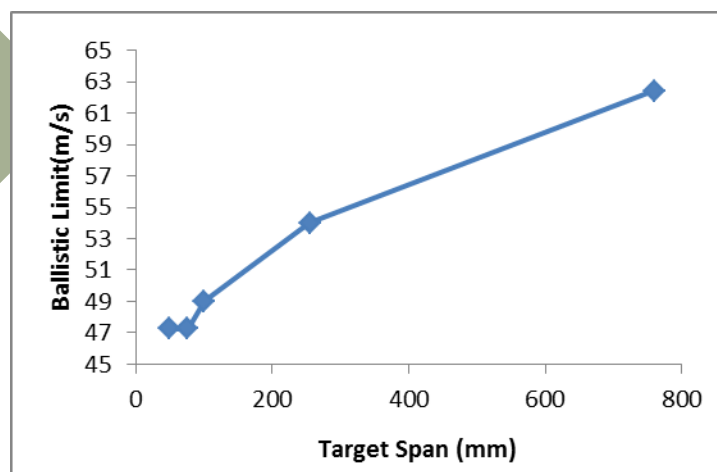


Figure 11: Variation of ballistic limit with the target span diameter

The ballistic limit of 760 mm span diameter was found to be 13.4%, 21.4%, 24.2% and 24.24% higher than that of the 255 mm, 100 mm, 76 mm and 50 mm span diameter respectively. The reason behind such behavior is the energy absorbed in bending that is higher for a larger span diameter.

For each target span the plastic deformation was found to increase with the decrease in projectile impact velocity such that the highest plastic deformation was found at ballistic limit. It was also observed that the plastic deformation of target increased with an increase in target span diameter. This is the fact due to which the ballistic limit increased with an increase in target span diameter.

Conclusion:

Three-dimensional numerical simulations were performed wherein ogive nosed projectiles were hit normally on 1 mm thick 1100-H12 aluminum target with varying configuration and span diameter.

The ballistic limit of monolithic target was found to be 17.7% and 25.8% higher than the double layered in-contact and 2 mm spaced target respectively. The ballistic limit of layered in-contact target was found to be 7% higher than 2 mm spaced target. The variation of spacing had insignificant effect on the ballistic limit.

The ballistic limit velocity consistently increased with an increase in target span diameter. The increase in ballistic limit occurred due to the increase in bending energy. The ballistic limit of 760 mm span diameter was found to be 13.4%, 21.4%, 24.2% and 24.24% higher than that of the 255 mm, 100 mm, 76 mm and 50 mm span diameter respectively.

References:

- [1] N.K. Gupta, M.A. Iqbal, G.S. Sekhon, Experimental and numerical studies on the behavior of thin aluminum plates subjected to impact by blunt and hemispherical-nosed projectiles, *International Journal of Impact Engineering*, 32(2006)1921-1944.
- [2] M.A. Iqbal, A. Chakrabarti, S. Beniwal, N.K. Gupta, 3D numerical simulations of sharp nosed projectile impact on ductile targets, *International Journal of Impact Engineering*, 37(2010)185–195.

- [3] A. Arias, J.A. Rodriguez-Martinez, A. Rusinek, Numerical simulations of impact behavior of thin steel plates subjected to cylindrical, conical and hemispherical non-deformable projectiles, *Eng Fract Mech.* 75(2008) 1635–56.
- [4] N.K. Gupta, M.A. Iqbal, G.S. Sekhon, Effect of projectile nose shape, impact velocity and target thickness on deformation behavior of aluminum plates, *Int. J. Solids and Str.* 44(2007) 3411–3439.
- [5] N.K. Gupta, M. A. Iqbal, G.S. Sekhon, Effect of Projectile nose shape, impact velocity and target thickness on the deformation behavior of layered plates. *Int. J. Impact Engng* 35(2008) 37-60.
- [6] R.S. Corran, P.J. Shadbolt, C. Ruiz, Impact loading of plates – an experimental investigation. *International Journal of Impact Engineering* 1 (1983), 3–22
- [7] J. Dean, C.S. Dunleavy, P.M. Brown, T.W. Clyne, Energy absorption during projectile perforation of thin steel plates and the kinetic energy of ejected fragments. *International Journal of Impact Engineering* 36, (2009)1250-1258.
- [8] ABAQUS/Explicit user's manual. Version 6.7: vol. 1(2), 2007.
- [9] G. R. Johnson, and W. H. Cook, A constitutive model and data for metals subjected to large strains, high strain rates and high temperatures. *Proc. the seventh International symposium on Ballistics*, The Hague. 1983
- [10] G. R. Johnson, and W. H. Cook. Fracture characteristics of three metals subjected to various strains, strain rates, temperatures and pressures. *Eng Fract Mech.*, 21(1985) 31-48.
- [11] R. A. Westmann. *J. Math Physics* 43(1964)191-198.
- [12] J. Awerbuch, S.R. Bodener, Analysis of the mechanics of perforation of projectile in metallic plates. *International Journal of Solids and Structures* 10(1973) 671-684.
- [13] R. F Recht, T. W. Ipson, *Appl. Mech.. Trans. ASME*, 30(1973)384.
- [14] M.E Backman, W. Goldsmith, The mechanics of penetration of projectile into targets. *International Journal of Engineering Science* 16(1978)1-99.
- [15] M.L. Wilkins,. Mechanics of Penetration and perforation. *International journal of Impact Engineering* 16(1978)793-807.

Table 1 Material parameters for 1100-H12 aluminum

Modulus of Elasticity, E (N/mm ²)	65762
Poisson's Ratio, ν	0.3
Density, ρ (kg/m ³)	2700
Yield Stress, A (N/mm ²)	148.361
B (N/mm ²)	345.513
n	0.183
Reference Strain Rate, $\dot{\epsilon}_0$ (s ⁻¹)	1.0
C	0.001
m	0.859
T _{melt} (K)	893
T ₀ (K)	293
Specific Heat, C _p (J/kg-K)	920
Inelastic heat fraction, α	0.9
D ₁	0.071
D ₂	1.248
D ₃	-1.142
D ₄	0.0097
D ₅	0.0

Table 2 Experimental and numerical results for varying configuration of 1 mm thick target impacted by ogive nosed projectile

Total Target Thickness = 1 mm, Span Diameter = 255 mm						
Ogive Nosed Projectile of (Mass = 52.5 grams, Diameter = 19 mm)						
Experimental Results Gupta et al. [5]		3D Numerical Results of Present Study				
Impact Velocity V _i (m/s)	Double Layered Target	Monolithic Target	Layered in contact Target	Spaced Target		
				2 mm	5 mm	10 mm
Residual Velocity (m/s)						
116.19	104.96	102.27	104.83	107.6	107.7	107.6
110.44	96.91	96.21	98.85	101.3	101.4	101.3
103.52	85.87	88.19	91	93.5	93.6	93.5
95.26	73.99	74.52	81.7	84.3	84.4	84.4
89.55	64.49	66.33	74.56	77.6	77.7	77.7
85.61	56.89	62.87	68.26	73.2	73.18	73.2

77.4	43.26	53.1	59.54	62.8	62.71	62.8
64.46	25.35	32.19	40.76	45.5	45.6	45.7
60	-	14.31	-	-	-	-
54.77	12	-	22.39	31	31	30.7
53	-	0				
50	-	-	12.58	-	-	-
46	-	-	0	6.36	6.73	7.19
45	-	-	-	1.5	1.9	2.1
44	-	-	-	0	0	0
41.3	-	-	-	-	-	-
39.18	0	-	-	-	-	-

Table 3 Experimental and Numerical results for 1 mm thick monolithic target with varying span diameter impacted by ogive nosed projectile

Target Thickness = 1 mm							
Ogive Nosed Projectile (Mass = 52.5 gms , Diameter = 19 mm)							
	Experimental Results Gupta et al.[5]	Axi-Symmetric Numerical Results Gupta et al.[5]	3D Numerical Results of Present Study				
	Span Diameter (mm)						
Impact Velocity V_i (m/s)	Residual Velocity (m/s)						
	255	50	76	100	255	760	
112.72	99.11	95.64	99.2	97.61	96.85	95.14	94.34
97.23	78.26	73.25	83.05	82.33	80.91	79.69	79.29
82.97	61.62	55.71	66.89	65.82	65.09	61.54	60.16
81.91	58.19	53.27	65.3	64.7	64.17	60.45	59.33
73.3	44.38	38.67	52.33	51.32	50.66	45.4	38.12
65.8	29.68	26.04	40.41	38.56	37.3	27.03	17.67
59	-	-	32.64	31.42	30.83	13.96	0
58.85	-	-	32.54	30.95	29.78	13.13	
57.28	17.86	15.93	29.73	28.68	27.64	12.12	-
55.5	-	-	27.73	26.09	24.55	6.62	-
52.5	-	-	21.32	20.27	18.4	0	-
52.1	-	0	20.01	18.32	16.19	-	-
51.6	-	-	19.16	17.17	15.13	-	-
51.27	8.72	-	18.2	15.41	12.7	-	-
50	-	-	14.25	11.83	9.2		

48	-	-	5.2	3.2	0	-	-
46.5	-	-	0	0	-	-	-
45.3	0	-	-		-	-	-

Table 4 Ballistic limit of different configurations of 1 mm thick target

Target Configuration	Ballistic Limit (V_{50} m/s)
	Ogive Nosed Projectile
Monolithic	56.5
Double layered in Contact	48.0
2 mm spacing	44.9
5 mm spacing	44.6
10 mm spacing	44.5
20 mm spacing	44.5
30 mm spacing	44.5

Table 5 Ballistic limit of 1 mm thick monolithic target with varying span diameter

Target Span Diameter (mm)	Ballistic Limit (V_{50} m/s)
50	47.25
76	47.25
100	49.0
255	54.0
760	62.4